Drug Development and Industrial Pharmacy, 2009; 35(10): 1201–1209

informa
healthcare

ORIGINAL ARTICLE

The influence of porosity changes in human epidermal membrane during iontophoresis on the permeability enhancement of a model peptide

Hugh D.C. Smyth[1], Gordon Becket[2] and Samir Mehta[3]

[1]Division of Pharmaceutical Sciences, College of Pharmacy, University of New Mexico, Albuquerque, NM, USA, [2]School of Pharmacy and Pharmaceutical Sciences, The Faculty of Science and Technology, University of Central Lancashire, Preston, Lancashire, UK and [3]Intas Pharmaceuticals Inc., Raleigh, NC, USA

Abstract

Purpose: We tested the hypothesis that the increases in the porosity of the skin during iontophoresis would not significantly increase the transport of peptides due to the small size of electrically induced pores. To investigate this mechanistically, we used human epidermal membrane under constant voltage conditions, applying the Nernst–Planck equation to the transport of a small ionic solute, tetraethylammonium bromide (TEAB), and a model peptide, luteinizing hormone releasing hormone. *Methods*: Steady-state flux of the drugs was determined under passive conditions and also during iontophoresis using constant DC voltages applied across side-by-side diffusion cells. Electrical conductance measurements were used to monitor the porosity changes that occur during electrical field application. *Results*: Porosity increases observed in the membrane substantially increased the permeability enhancement of the small ionic solute TEAB. The permeability enhancement was well described by Nernst–Planck model predictions after porosity changes in the membrane were taken into account. Enhancement of luteinizing hormone releasing hormone under identical conditions was much less than TEAB. The porosity increases induced by iontophoresis had little or no effect on the permeability enhancement of the larger molecule. *Conclusions*: These findings closely parallel those reports that have found electrically induced pores to be significantly smaller than preexisting pores in the human epidermal membrane. The data obtained also support the view that iontophoresis-induced pores, alone, may provide limited benefit for macromolecule transport across the skin.

Key words: *Hindered pore theory; human epidermal membrane; luteinizing hormone releasing hormone; Nernst–Planck model; skin porosity; transdermal drug delivery*

Introduction

Many new peptide and protein drugs continue to be developed by the biotechnology industry. Such molecules are very promising therapeutically due to their specificity and potency. However, widespread development of such medicines is impeded by their special drug characteristics including challenging delivery requirements. In this respect, transdermal delivery has several potential benefits for peptide administration over currently employed methods[1]. Delivering compounds across the skin bypasses the proteolytic degradation in the gastrointestinal tract and first pass effect has potential for controlling release profiles, and rapid cessation of therapy is easily performed[2]. In addition, the noninvasive nature of transdermal delivery improves patient acceptability relative to the current practice of administering these compounds via injection[3]. However, despite the recent interest in the field of transdermal peptide delivery, the skin is well recognized as an excellent barrier to peptide molecules that are generally large and hydrophilic[4]. Numerous efforts to increase the permeability of the skin barrier have been reported[5]. The large majority

Address for correspondence: Dr. Hugh D.C. Smyth, Division of Pharmaceutical Sciences, College of Pharmacy, University of New Mexico, MSC 09 5360, Albuquerque, NM 87131, USA. Tel: +1 505 272 2939, Fax: +1 505 272 6749. E-mail: hsmyth@salud.unm.edu

(Received 16 Sep 2008; accepted 4 Mar 2009)

ISSN 0363-9045 print/ISSN 1520-5762 online © Informa UK, Ltd.
DOI: 10.1080/03639040902865673

of literature in this area focuses on the use of chemical penetration enhancers and electrically assisted transdermal delivery. Recently, we also investigated the potential of combining chemical permeation enhancers with iontophoresis to increase the delivery of a model peptide[6]. As such, one of the most promising methods in terms of peptide delivery is iontophoresis. The fundamental concepts of iontophoresis have been well described in the literature[7]. A small electrical potential (<10 V) is applied across the skin as a driving force to increase drug permeation. Three main mechanisms can promote drug delivery in iontophoresis. First, charged species, contained within an electrolyte solution, move down their electromotive gradient across the stratum corneum. Second, an electroosmotic solvent flow occurs across the skin and assists in the delivery of some solutes during electrical field application[8]. Third, iontophoresis assists permeation by inducing structural changes in the skin during the application of moderate electrical potential gradients (>1 V)[9]. These structural alterations appear to resemble the formation of new pathways similar to those created during electroporation[9–11]. Electroporation of the stratum corneum requires much larger voltages (>50 V) to create new pores in the lipid bilayers of the intercellular matrix[12,13]. However, the presence of shunt pathways with much less lipid bilayer resistance has given rise to the idea of pores forming in the lining of appendages termed 'macropores'[13,14]. Recent thermodynamic investigations into the nature of induced pores have reported that the size of these pathways appears to be smaller than the preexisting pores (10Å versus 20Å, respectively)[15]. The similar size of the voltage-induced pathways in the skin and peptide molecules may mean that iontophoretic permeation enhancement will be significantly restricted through these new pathways. To date no investigations designed to address this issue using large solutes have been reported. In these studies, we employ a peptide, luteinizing hormone releasing hormone (LHRH), a well-characterized molecule used in multiple in vitro and in vivo studies[16–20]. Moreover, we use constant voltage iontophoresis across human skin[21]. This approach allows us to employ the modified Nernst–Planck equation to probe permeability of various solutes on a mechanistic level[21–23].

The purpose of this study was to investigate the hypothesis that increases in the porosity of the Human epidermal membrane (HEM) will not significantly increase the transport of peptides due to the small size of electrically induced pores. Specifically, we compared the permeability enhancement of LHRH to the enhancement of a small ionic solute tetraethylammonium bromide (TEAB) under the same experimental conditions.

Model development and experimental strategy

Constant voltage iontophoresis allows easy application of the Nernst–Planck equation for electrochemical transport phenomena. The modified Nernst–Planck equation (Equation 1) provides a general framework for mechanistic iontophoresis transport studies[11,15,24]. The applied model expresses iontophoretic transport in terms of the passive diffusion, migration driven by electric field, and electroosmotic flow contributions[11].

$$J_{\Delta\psi} = -\varepsilon\left\{HD\left[\frac{\mathrm{d}C}{\mathrm{d}x} + \frac{CzF}{R_{\mathrm{gas}}T}\frac{\mathrm{d}\psi}{\mathrm{d}x}\right] \pm WvC\right\}, \qquad (1)$$

where ψ is the electrical potential across the membrane, F is the Faraday constant, R_{gas} is the gas constant, T is the temperature, v is the average velocity of the convective solvent flow, ε is the combined porosity and tortuosity factor of the membrane, C is the concentration, x is the position in the membrane, z is the charge number, D is the diffusion coefficient of the permeant, H and W are hindered transport factors, and J is the flux of the species in one dimension.

Certain limitations arise when attempting to apply this theory to the experimental protocols that were used here. First, LHRH molecular size is close to that of the pore size estimates; therefore it is necessary to account for steric interactions between the solute and the membrane using the hindered pore theory[10]. Hindered transport factors are used to account for the differences in the size of the model solutes relative to the pore dimensions. In effect, the hindrance factors reduce the free diffusion coefficient of a solute to the diffusion coefficient of the molecule in a cylindrical pore. An extensive review of the hindered pore theory can be found in the literature[25]. Our experimental strategy incorporated the hindered pore theory by calculating the Stokes radii of the solutes. Molecular weight gives an indication of relative sizes of molecules, but it is of limited use in predictions for transport studies. In the case of large molecules, molecular weight values do not convey information on the hydrodynamic properties of solutes. These type of molecules often experience intramolecular bonding and form complex tertiary structures that may not follow molecular weight to molecular volume correlations used for smaller molecules[26]. Therefore, for transport studies, size estimates from the diffusion coefficient and Stokes radius are preferred[27].

The Nernst–Planck equation (Equation 1) can be integrated to yield permeability enhancement ratios (E) for a particular solute. These are useful because they

allow easy comparison between two different types of molecules. In effect, they are simply the ratio of iontophoresis flux and passive flux (Equation 2):

$$E = \frac{J_{\text{ionto}}}{J_{\text{passive}}}. \tag{2}$$

Schematically, the enhancement ratio calculated from the Nernst–Planck model can be separated out into the following components contributing to overall enhancement (Equation 3)

$$E = E_{\text{ionto}} + E_{\text{electroosmosis}}. \tag{3}$$

Thus, dominant effects predicted by the model are the direct electrical field effect and electroosmosis forces[11].

The other main limitation of applying the Nernst–Planck model for transdermal iontophoresis experiments is the assumption that membrane barrier properties remain unchanged during electrical field application. Under an applied potential of around 1 V or greater, the porosity of the HEM increases[9]. At these voltage levels, the observed enhancement ratios can also be schematically represented by the contributing components of permeability enhancement (Equation 4):

$$E_{\text{observed}} = (E_{\text{ionto}} + E_{\text{electroosmosis}}) \times E_{\Delta R}, \tag{4}$$

where $E_{\Delta R}$ is the increase in porosity of the membrane due to the electrical field. $E_{\Delta R}$ represents the change in ε, the porosity–tortuosity factor, from the Nernst–Planck equation (Equation 1). To facilitate comparisons between the observed E ratio obtained from iontophoretic flux studies (Equation 4) and the E ratio derived from the Nernst–Planck model (Equation 3), the membrane permeability changes that occur during iontophoresis experiments must be taken into account. Electrical conductance changes provide a good estimate of porosity changes[9,11,14,15]. Therefore, increases in porosity, $E_{\Delta R}$, can be estimated by changes in HEM electrical conductance (G)[15],

$$E_{\Delta R} \approx \frac{G_{\text{ionto}}}{G_{\text{passive}}}, \tag{5}$$

giving

$$E_{\text{model}} \times E_{\Delta R} = E_{\text{expected}}; \tag{6a}$$

therefore,

$$E_{\text{expected}} \approx E_{\text{observed}}. \tag{6b}$$

This relationship (Equation 6b) is valid if the porosity increases provide additional transport pathways for the solute under investigation. Conductance, being a measure of the electromobility of the background electrolyte in the HEM, is more likely to indicate the porosity changes for ions that are similar in size to sodium and chloride ions (the primary conducting ions)[11]. Therefore, if the voltage-induced pores, as indicated by conductance changes, are smaller than the permeant dimensions, then correcting for porosity will fail to fit the model predictions to the observed enhancement ratios. This approach allows the effect of the porosity changes on the transport of different-sized ions to be analyzed at moderate iontophoresis voltages.

Methods

Materials

Radiolabeled [^{3}H]LHRH, [^{14}C]TEAB, and [^{14}C]sucrose were obtained from New England Nuclear (Boston, MA, USA). Phosphate-buffered saline (PBS) (pH 7.4) was obtained from Sigma Chemical Co. (St. Louis, MO, USA). Silver wire (99.9% purity) was also obtained from Sigma Chemical Co. Lengths of silver wire (15 cm) were coiled and used as electrodes. To obtain a silver chloride electrode, the coiled silver wire was electroplated in 3 M KCl. All other chemicals used were of analytical grade. Deionized water (resistivity >18 MΩ cm) was used to prepare all solutions. Full-thickness human skin samples from female abdominal, breast, or lower back skin were obtained from the International Institute for the Advancement of Medicine (IIAM; Scranton, PA, USA).

Determination of Stokes radii

The diffusion coefficients (D) of the permeants were determined using fritted glass diffusion cells as previously described[27]. In our experiments, glass side-by-side diffusion cells were used and a fritted glass disk (type F, pore size ≈ 5 μm; Ace Glass, Vineland, NJ, USA) was tightly positioned between the donor and the receptor compartments. The donor solution for LHRH required the addition of 'cold' LHRH to the trace amounts of radiolabeled LHRH in solution to minimize the effect of peptide adsorption to binding sites on the fritted glass and enabled steady-state permeability coefficients to be determined. Diffusion coefficients were determined by using the following equation[27]:

$$P = \frac{\varepsilon D_r}{\tau h}, \tag{7}$$

where P is the permeability coefficient; ε, τ, and h are the porosity, tortuosity of the diffusional pathway, and

thickness of the membrane, respectively; and D_r is the diffusion coefficient of the permeant. The parameters ε, τ, and h were determined by calibrating the system with sucrose, for which the diffusion constant was taken from the literature[27]. The diffusion coefficient was then used in the Stokes–Einstein equation to calculate the Stokes radius, r, of each solute.

$$r = \frac{RT}{6\pi\eta ND}, \tag{8}$$

where η is the solvent viscosity, R is the gas constant, T is the absolute temperature, and N is Avogadro's number. Results reported by Nikiforovich and Marshall of several low-energy LHRH conformers were modeled using Weblab Viewer Lite®[28]. Manipulation of these 3D structures allowed measurements of distances within the structure and were compared to our Stokes radius results.

Preparation of epidermis

HEMs were prepared from full-thickness female abdominal, breast, or lower back skin. The epidermis was prepared using the widely described heat treatment method[29,30]. The tissue was stored at −60°C until required. Membranes to be used in diffusion experiments were allowed to thaw, placed in PBS, and allowed to hydrate at room temperature overnight. HEM samples were selected for their integrity using electrical resistance measurements [made at low potential difference (0.3 V) applied over short instances] in addition to visual inspection. Only samples with baseline resistance of greater than 20 kOhms/cm^2 were used in the permeability experiments.

In vitro HEM studies

The general procedure for performing in vitro permeability experiments has been well described in the literature[26,31]. In our study, sheets of HEM were mounted between the two side-by-side diffusion half cells, stratum corneum side facing the donor compartment. The diffusion cells were firmly clamped leaving an area exposed for diffusion of 0.64 cm^2. The compartment volumes (3 mL) were each maintained at 37°C and stirred using small Teflon-coated magnetic bars.

All permeability measurements were performed in 0.1 M PBS solutions at pH 7.4. Iontophoresis treatments involved applying a constant DC voltage across the membrane at preselected levels (1, 2, 3, and 4 V) using Scepter©, a computer-controlled power supply. Regular sampling from the receptor allowed the calculation of flux for each permeant. These samples were mixed thoroughly with 5 mL of liquid scintillation fluid (Ultima Flo M™, Packard, Meriden, CT, USA) and analyzed in a Beckman LS5801 scintillation counter for 10 minutes. The sensitivity of liquid scintillation counting enabled low concentrations of the radiolabeled permeants to be present in the donor solution whilst ensuring that there were no osmotic pressure contributions and solute–solute interactions were negligible.

During the course of all experiments, including those without iontophoretic currents applied, electrical conductance measurements of the membranes were monitored. These conductance measurements were utilized in the estimation of membrane porosity changes that occur at moderate iontophoretic voltages as outlined in Model Development and Experimental Strategy.

Data analysis

Distintegrations per minute (DPM) counts measured for each receptor sample were converted to amounts of compound using the specific activity, dilution, and sampling corrections. Plots of cumulative amount, Q, over time, t, were subsequently constructed. From these, permeability coefficients (normalized flux), P, for each solute was determined using the following equation[27]

$$P = \frac{1}{A\Delta C}\frac{\mathrm{d}Q}{\mathrm{d}t}, \tag{9}$$

where $\mathrm{d}Q/\mathrm{d}t$ is the steady-state slope of the above-mentioned plots, A is the diffusional area, and ΔC is the concentration difference across the membrane. The permeability coefficients were then used to calculate enhancement ratios for each treatment group. Enhancement ratios were calculated by dividing the permeability coefficient of the solute resulting from iontophoresis by the permeability observed during passive conditions:

$$E_{\text{observed}} = \frac{P_{\text{iontophoresis}}}{P_{\text{passive}}}. \tag{10}$$

The experimental enhancement ratios, E_{observed}, were compared to enhancement ratios calculated using the modified Nernst–Planck equation (Equation 1), E_{model}. In the model, the contribution of electroosmosis to a solute flux enhancement is represented by the Peclet number, Pe[11]. The Pe contributions were estimated by incorporating a nonionic solute into the iontophoresis experiments since convective solvent flow velocity is particularly troublesome to calculate in complex systems such as the HEM[8,32]. Under Ohmic conditions, nonionic solutes will not be influenced by direct repulsion forces from the electrical field and therefore are representative of electroosmosis effects only[11].

The E ratio for a nonionic molecule during iontophoresis is equivalent to its Peclet number[9,11]. Obtaining this value allows the calculation of Pe numbers for LHRH and TEAB using the equation derived by Li et al.[33] (Equation 11)

$$\mathrm{Pe}_{\mathrm{LHRH}} = \left(\frac{W_{\mathrm{LHRH}} H_{\mathrm{sucrose}} D_{\mathrm{sucrose}}}{W_{\mathrm{sucrose}} H_{\mathrm{LHRH}} D_{\mathrm{LHRH}}} \right) \mathrm{Pe}_{\mathrm{sucrose}}. \quad (11)$$

Results

Solute characteristics

LHRH, TEAB, and sucrose diffusion coefficients are displayed in Table 1. Distances across the backbone structure of low-energy conformers of LHRH, measured using Labviewer Lite®, and data from Nickovovich and Marshall ranged from 14.8Å to 20.5Å[28].

Observed enhancement ratios

The E ratio results from iontophoresis experiments for both LHRH and TEAB are summarized in Table 2. The experimental LHRH permeation enhancement ratios, E_{observed}, increased as the electrical field strength was increased, from 2.5-fold enhancement at 1 V to 13.5-fold enhancement at 4 V (Table 2 and Figure 1). Similarly, TEAB enhancement ratios were observed to increase as the electrical field strength increased (Figure 2). However, the magnitude of TEAB enhancement ratios was three orders of magnitude greater than the LHRH-observed enhancement ratios. Identical sucrose iontophoresis experiments were also performed to allow the estimation of the convective solvent flow component of iontophoretic permeation enhancement. In accordance with TEAB and LHRH observations, sucrose permeation enhancement also increased with electrical field strength (Figure 3).

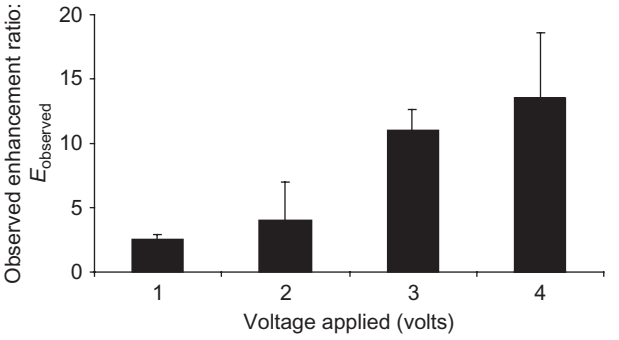

Figure 1. Observed enhancement ratios for LHRH, E_{observed}.

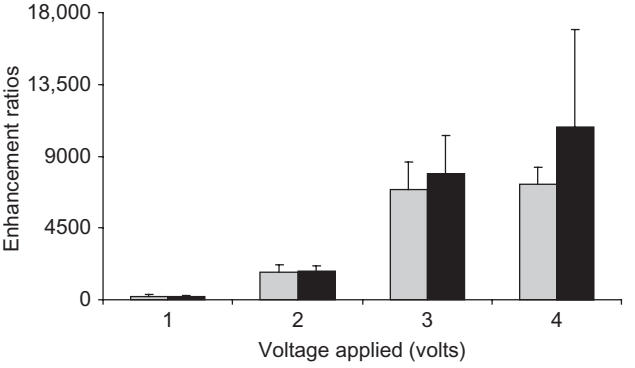

Figure 2. Observed enhancement ratios for TEAB, E_{observed} (gray bars), and expected enhancement ratios, E_{expected}, as calculated from Equation (6a) combining the Nernst–Planck model and porosity changes (black bars).

Table 1. Diffusion coefficients and Stokes radii for solutes used.

Compound	Molecular weight	Diffusion coefficient (10^{-6} cm^2/s)	Stokes radius (Å)
TEAB[a]	131	8.7	3.75
LHRH[a]	1182.5	1.4	23.7
Sucrose[b]	342	6.98	5.55

[a]Experimentally determined in this study. [b]Determined by fritted glass experiment[27,34].

Table 2. Permeation enhancement ratios.

Permeant	Voltage (volts)	Observed permeability enhancement ratios: E_{observed}[a]	Porosity increases: $E_{\Delta R}$[a]	Nernst–Planck model enhancement ratio: E_{model}[b]	Expected enhancement ratio ($E_{\mathrm{model}} \times E_{\Delta R}$): E_{expected}[a]
TEAB	1	181 ± 140	5.3 ± 1.6	40	209.9 ± 63.4
	2	1732 ± 469	22.5 ± 4.1	79	1770.8 ± 322.7
	3	6938 ± 1718	66.9 ± 20.5	118	7874.1 ± 2412.8
	4	7212 ± 1091	69.0 ± 38.9	157	10,812.3 ± 6095.6
LHRH	1	2.5 ± 0.4	5.2 ± 1.3	231	2233 ± 1638
	2	4.0 ± 3.0	9.4 ± 4.5	408	3816 ± 1827
	3	11.0 ± 1.6	25.9 ± 9.2	584	15,133 ± 5358
	4	13.5 ± 5.1	98.8 ± 72.6	761	75,145 ± 55,243

[a]Mean ± SD, $n \geq 4$. [b]Calculated from modified Nernst–Planck equation using 30Å as effective HEM pore radius.

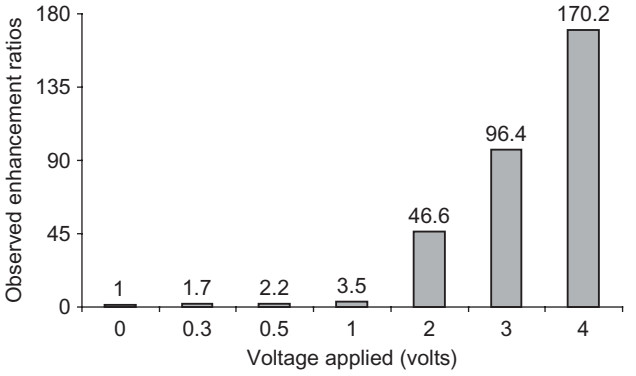

Figure 3. Observed enhancement ratios for sucrose, the electroosmotic flow marker.

Electrical conductance measurements

Electrical conductance changes, $E_{\Delta R}$, were also measured to assist in predicting the porosity changes that occur in the membrane. These are also summarized in Table 1. Like the E ratios, electrical conductance of the membrane increased as electrical field strength was increased in both the LHRH and the TEAB experiments. A maximum increase in $E_{\Delta R}$ was detected at 4 V for both experiment groups although the standard deviation was large.

Nernst–Planck enhancement ratios

The Nernst–Planck model enhancement ratios, E_{model}, were calculated assuming a 30Å pore radius for each solute using methods described in Model Development and Experimental Strategy (Table 2). The model enhancement ratios were transformed using Equation (6a) to obtain E_{expected}, an enhancement ratio that can be compared to the experimental enhancement ratios. A summary of E_{expected} values for LHRH is shown in Figure 4. These E_{expected} ratios are clearly several orders of magnitude greater than the observed permeation enhancement ratios (Figure 1). The expected enhancement ratios, E_{expected}, for TEAB are plotted on Figure 2.

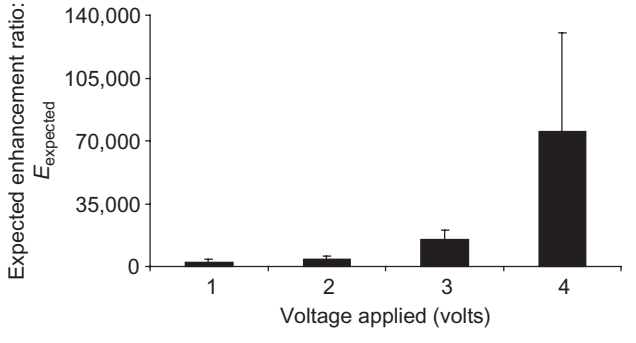

Figure 4. Expected enhancement ratios for LHRH (E_{expected}) as calculated from Equation (6a) combining the Nernst–Planck model and porosity changes.

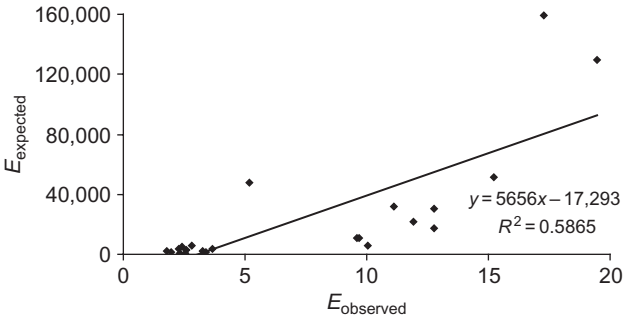

Figure 5. E_{expected} ratios for LHRH plotted against the respective enhancement ratios observed during iontophoresis experiments.

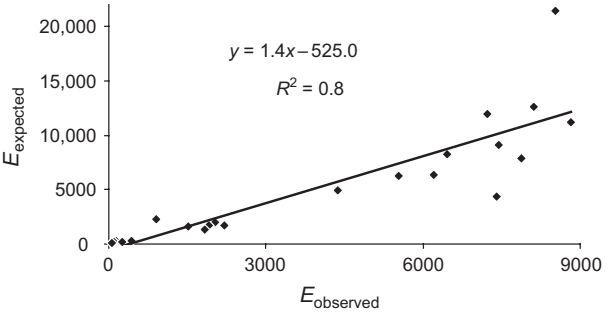

Figure 6. E_{expected} ratios for TEAB plotted against the respective enhancement ratios observed during iontophoresis experiments.

Unlike observations for LHRH, the E_{expected} compare well with the observed permeation enhancement ratios, E_{observed}. Figures 5 and 6 are scatter plots of E_{expected} versus E_{observed} for LHRH and TEAB, respectively. This representation facilitates a comparison of the observed values with the expected model predictions. An identical match between the model and observations would be represented by a slope of 1 between this data. For LHRH, the slope is 5656, demonstrating a large discrepancy between the observed permeation enhancement and that predicted by the model. Conversely, TEAB results show a slope of approximately 1.4, representative of excellent agreement between the data sets.

Discussion

Solute selection and characterization

LHRH is a good example of a peptide that has been well studied and has good stability[35]. Stokes–Einstein measurements demonstrated that LHRH has an approximate radius of 23Å. A molecule with these dimensions was selected because the effective pore size in the HEM is reported to be close to this value (20–30Å)[11,36]. Therefore, in studies exploring possible changes in pore size

of the HEM, the transport of LHRH is likely to be a good marker for such alterations. The LHRH hydrodynamic radius determined by diffusion studies falls in the same order of magnitude as the size of low-energy molecular modeling estimations[28]. TEAB was the small ionic solute used for comparison (radius ~4Å). This compound has also been used in transdermal iontophoresis studies and is well characterized[11,30]. Our observed LHRH permeability during iontophoresis ranged from approximately 6×10^{-4} to 6.4×10^{-3} cm/h. The permeability coefficients of LHRH appear to fit well with those previously reported[30,37]. In vitro LHRH iontophoresis permeability results have been described by Bhatia et al.[37] These studies were performed using skin from various species under several different experimental treatments. It is important to recognize that skin permeability varies considerably between species and significant variation is even seen within the same patient. Despite these known differences, iontophoresis permeability coefficients reported were in the range of 1×10^{-3}–1×10^{-4} cm/h and therefore in agreement with our observations. In previous investigations, LHRH permeability across human skin was below the limits of high-performance liquid chromatography detection[38,39] whilst in animal studies, LHRH permeability appeared to be measurable[24,29]. Our laboratory used intact human tissue that is generally reported to have lower permeability relative to animal skin for many solutes[40,41] and therefore necessitated the use of radioalabeled LHRH and liquid scintillation counting as an analytical method. Reports of TEAB permeability coefficients in HEM are also in the literature (passive permeability from around 5×10^{-5} to about 8×10^{-4} cm/h)[30]. These are similar to the passive permeability coefficients observed for TEAB in this study (5.9×10^{-5}–1.2×10^{-4} cm/h).

Calculation of $\mathbf{E}_{model}$

The Pe number from Equation (11) was calculated using the linear relationship between electroosmotic flow and voltage below 1 V. In this voltage region, Pe is directly proportional to electrical field strength (Figure 3)[8,32,42]. Using this methodology, we avoided any bias introduced into electroosmotic flow transport by the structural and porosity changes that occur in the membrane at voltages above 1 V. Once Pe values are known, the theoretical enhancement ratio was easily calculated and was compared to observed E ratios corrected for observed porosity changes.

Porosity effects on solute enhancement

The hypothesis that voltage-induced pores during moderate voltage iontophoresis are too small to provide additional pathways for macromolecule transport was the focus of our studies. By combining porosity change measurements with permeability enhancement data for a small and a large solute, we were able to provide experimental support for this proposal. TEAB permeability, E_{observed}, increased dramatically as the porosity of the membrane, $E_{\Delta R}$, also increased during iontophoresis (Table 2). However, porosity increases observed during LHRH iontophoresis had a much smaller effect on LHRH permeability enhancement.

To calculate the proportion of TEAB permeability enhancement resulting from electrically induced changes in the membrane, the observed permeability data were compared to the theoretical model (Table 2). It was apparent that the observed permeability enhancement ratios were in general an order of magnitude greater than E_{model} predictions when porosity changes were not taken into account. By incorporating the porosity changes ($E_{\Delta R}$) into the Nernst–Planck model predictions, the expected enhancement ratio, E_{expected} (enhancement expected if voltage-induced porosity changes give rise to new pathways for solute transport), was derived. For TEAB, excellent agreement of E_{expected} with E_{observed} indicates that the differences between the observed enhancement ratio and the Nernst–Planck-derived predictions (E_{model}) are for the most part explained by porosity increases (Figure 5). Examination of the LHRH permeability data shows a large disagreement between the E_{observed} ratios and the model enhancement ratios, E_{model} (Table 2). Furthermore, incorporating the porosity correction created an even greater discrepancy between E_{observed} and the Nernst–Planck model (Table 2, Figure 6). From these comparisons and in light of TEAB results, it appears that the electrically induced changes in the membrane did not influence LHRH enhancement to the same extent observed with TEAB. We cannot infer from our data that there was any increase in permeability enhancement of LHRH due to voltage-induced pathways. However, if LHRH permeability is enhanced by voltage-induced pathways, the magnitude of enhancement is considerably smaller than that observed for TEAB.

Our observations provide experimental support to studies that have looked at the nature of these voltage-induced pores[15]. These researchers predicted the induced pathways to be around 10Å in radius, much smaller than the radius of the existing pores (20Å). Pores of this size are unlikely to be of significant benefit in promoting the transport of many protein and peptide drugs that have molecular dimensions in this order of magnitude.

Conclusions

During moderate voltage iontophoresis the skin porosity increased, as indicated by increases in the electrical

conductance of the membrane. The porosity increases promoted the permeability of TEAB, a small ionic solute. By applying a correction for porosity changes, it was possible to compare observed permeation enhancement ratios for TEAB to the modified Nernst–Planck model predictions. Given the use of innately variable biological membranes, good agreement for TEAB was achieved. Enhancement of LHRH during moderate voltages was much less than that observed for TEAB. Porosity increases appeared to have insignificant influences on LHRH permeability. Applying the porosity correction did not provide agreement between observed enhancement data and the modified Nernst–Planck equation. Overall, iontophoretic transport of the larger LHRH molecule was significantly more restricted than the small ionic solute TEAB. Thus, our hypothesis that increases in the porosity of the HEM will not significantly increase the transport of peptides due to the small size of electrically induced pores is supported by this direct and mechanistic analysis in HEM.

Acknowledgments

Supported by GlaxoWellcome Inc. (Research Triangle Park, NC, USA) and Vernon Tews Pharmacy Postgraduate Education Scholarship, New Zealand.

Declaration of interest: The authors report no conflicts of interest.

References

1. Benson HA, Namjoshi S. (2008). Proteins and peptides: Strategies for delivery to and across the skin. J Pharm Sci, 97(9):3591–610.
2. Batheja P, Thakur R, Michniak B. (2006). Transdermal iontophoresis. Expert Opin Drug Deliv, 3(1):127–38.
3. Li GL, Van Steeg TJ, Putter H, Van Der Spek J, Pavel S, Danhof M, et al. (2005). Cutaneous side-effects of transdermal iontophoresis with and without surfactant pretreatment: A single-blinded, randomized controlled trial. Br J Dermatol, 153:404–12.
4. Brown MB, Traynor MJ, Martin GP, Akomeah FK. (2008). Transdermal drug delivery systems: Skin perturbation devices. Methods Mol Biol, 437:119–39.
5. Amsden BG, Goosen MFA. (1995). Transdermal delivery of peptide and protein drugs—An overview. AIChE J, 41(8): 1972–97.
6. Smyth HDC, Becket G, Mehta SC. (2002). Effect of permeation enhancer pretreatment on the iontophoresis of luteinizing hormone releasing hormone (LHRH) through human epidermal membrane (HEM). J Pharm Sci, 91(5):1296–307.
7. Wong O. (1994). Iontophoresis: Fundamentals. In: Hsieh DS, ed. Drug permeation enhancement: Theory and applications. New York: Marcel Dekker, 219–46.
8. Pikal MJ. (1992). The role of electroosmotic flow in transdermal iontophoresis. Adv Drug Deliv Rev, 9(2–3):201–37.
9. Inada H, Ghanem AH, Higuchi WI. (1994). Studies on the effects of applied voltage and duration on human epidermal membrane alteration/recovery and the resultant effects upon iontophoresis. Pharm Res, 11(5):687–97.
10. Li SK, Ghanem AH, Peck KD, Higuchi WI. (1999). Pore induction in human epidermal membrane during low to moderate voltage iontophoresis: A study using AC iontophoresis. J Pharm Sci, 88(4):419–27.
11. Higuchi WI, Li SK, Ghanem AH, Zhu H, Song Y. (1999). Mechanistic aspects of iontophoresis in human epidermal membrane. J Control Release, 62(1–2):13–23.
12. Singh J, Dinh SM, Berner B. (1998). Electrical properties of skin. In: Berner B, Dinh SM, eds. Electronically controlled drug delivery. Boca Raton (FL): CRC Press, 47–62.
13. Prausnitz MR. (1997). Reversible skin permeabilization for transdermal delivery of macromolecules. Crit Rev Ther Drug Carrier Syst, 14(4):455–83.
14. Chizmadzhev Y, Indenbom A, Kuzmin P, Galichenko S, Weaver J, Potts R. (1998). Electrical properties of skin at moderate voltages: Contribution of appendageal macropores. Biophys J, 74(2 Pt 1):843–56.
15. Li SK, Ghanem AH, Peck KD, Higuchi WI. (1998). Characterization of the transport pathways induced during low to moderate voltage iontophoresis in human epidermal membrane. J Pharm Sci, 87(1):40–8.
16. Schuetz YB, Naik A, Guy RH, Vuaridel E, Kalia YN. (2005). Transdermal iontophoretic delivery of triptorelin in vitro. J Pharm Sci, 94:2175–82.
17. Schuetz YB, Naik A, Guy RH, Kalia YN. (2005). Effect of amino acid sequence on transdermal iontophoretic peptide delivery. Eur J Pharm Sci, 26:429–37.
18. Raiman J, Koljonen M, Huikko K, Kostiainen R, Hirvonen J. (2004). Delivery and stability of LHRH and Nafarelin in human skin: The effect of constant/pulsed iontophoresis. Eur J Pharm Sci, 21:371–7.
19. Kochhar C, Imanidis G. (2004). In vitro transdermal iontophoretic delivery of leuprolide under constant current application. J Control Release, 98:25–35.
20. Kochhar C, Imanidis G. (2003). In vitro transdermal iontophoretic delivery of leuprolide-mechanisms under constant voltage application. J Pharm Sci, 92:84–96.
21. Imanidis G, Luetolf P. (2006). An extended model based on the modified Nernst-Planck equation for describing transdermal iontophoresis of weak electrolytes. J Pharm Sci, 95:1434–47.
22. Li SK, Ghanem AH, Higuchi WI. (1999). Pore charge distribution considerations in human epidermal membrane electroosmosis. J Pharm Sci, 88:1044–9.
23. Li SK, Ghanem AH, Teng CL, Hardee GE, Higuchi WI. (2001). Iontophoretic transport of oligonucleotides across human epidermal membrane: A study of the Nernst-Planck model. J Pharm Sci, 90:915–31.
24. Sims SM, Higuchi WI, Srinivasan V. (1991). Skin alteration and convective solvent flow effects during iontophoresis. I. Neutral solute transport across human skin. Int J Pharm, 69:109–21.
25. Deen W. (1987). Hindered transport of molecules in liquid-filled pores. AIChE J, 33(9):1409–25.
26. Guy RH, Hadgraft J. (1989). Selection of drug candidates for transdermal delivery. In: Hadgraft J, Guy RH, eds. Transdermal drug delivery: Developmental issues and research initiatives. New York: Marcel Dekker, 59–81.
27. Peck KD, Ghanem AH, Higuchi WI. (1994). Hindered diffusion of polar molecules through and effective pore radii estimates of intact and ethanol treated human epidermal membrane. Pharm Res, 11(9):1306–14.
28. Nikiforovich G, Marshall G. (1993). Conformation-function relationships in LHRH analogs. I. Conformations of LHRH peptide backbone. Int J Pept Protein Res, 42(2):171–80.
29. Kligman A, Christophers E. (1963). Preparation of isolated sheets of human stratum corneum. Arch Dermatol, 88:702–5.
30. Sims SM, Higuchi WI, Srinivasan V. (1992). Skin alteration and convective solvent flow effects during iontophoresis. II. Monovalent anion and cation transport across human skin. Pharm Res, 9(11):1402–9.
31. Williams A, Barry B. (1992). Skin absorption enhancers. Crit Rev Ther Drug Carrier Syst, 9(3–4):305–53.
32. Peck KD, Srinivasan V, Li SK, Higuchi WI, Ghanem AH. (1996). Quantitative description of the effect of molecular size upon

electroosmotic flux enhancement during iontophoresis for a synthetic membrane and human epidermal membrane. J Pharm Sci, 85(7):781–8.
33. Li SK, Ghanem AH, Peck KD, Higuchi WI. (1997). Iontophoretic transport across a synthetic membrane and human epidermal membrane—A study of the effects of permeant charge. J Pharm Sci, 86(6):680–9.
34. Inamori T, Ghanem A, Higuchi WI, Srinivasan V. (1994). Macromolecule transport in and effective pore size of ethanol pretreated human epidermal membrane. Int J Pharm, 105(2):113–23.
35. Delgado-Charro MB, Guy RH. (1998). Iontophoresis of peptides. In: Berner B, Dinh SM, eds. Electronically controlled drug delivery. Boca Raton (FL): CRC Press, 129–57.
36. Ruddy SB, Hadzija BW. (1992). Iontophoretic permeability of polyethylene glycols through hairless rat skin: Application of hydrodynamic theory for hindered transport through liquid-filled pores. Drug Des Discov, 8(3):207–24.
37. Bhatia KS, Gao S, Singh J. (1997). Effect of penetration enhancers and iontophoresis on the FT-IR spectroscopy and LHRH permeability through porcine skin. J Control Release, 47(1):81–9.
38. Lu M, Lee D, Rao G. (1992). Percutaneous absorption enhancement of leuprolide. Pharm Res, 9(12):1575–9.
39. Srinivasan V, Su MH, Higuchi WI, Behl CR. (1990). Iontophoresis of polypeptides: Effect of ethanol pretreatment of human skin. J Pharm Sci, 79(7):588–91.
40. Cevc G. (1996). Transfersomes, liposomes and other lipid suspensions on the skin: Permeation enhancement, vesicle penetration, and transdermal drug delivery. Crit Rev Ther Drug Carrier Syst, 13(3–4):257–388.
41. Siddiqui O. (1989). Physicochemical, physiological, and mathematical considerations in optimizing percutaneous absorption of drugs. Crit Rev Ther Drug Carrier Syst, 6(1):1–38.
42. Peck KD, Hsu J, Li SK, Ghanem AH, Higuchi WI. (1998). Flux enhancement effects of ionic surfactants upon passive and electroosmotic transdermal transport. J Pharm Sci, 87(9):1161–9.